Application of fluids and promising materials as advanced inter-pane media in multi-glazing windows for thermal and energy performance improvement: A review

Yujian Huang, Mohamed El Mankibi, Richard Cantin, Mike Coillot

Version of Record: https://www.sciencedirect.com/science/article/pii/S0378778821007428
Manuscript_9b21438dd3e3830dddf38f95a8dafd32

Application of fluid and promising material as advanced inter-pane medium in multi-glazing windows for thermal and energy performance improvement: A review

Yujian Huang [a,*], Mohamed El Mankibi[a], Richard Cantin[b], Mike Coillot[a]

[a] *LTDS, ENTPE, Université of Lyon, 3 rue Maurice Audin, F-69120 Vaulx-en-Velin, France*

[b] *LGCB, ENTPE, Université of Lyon, 3 rue Maurice Audin, F-69120 Vaulx-en-Velin, France*

Abstract

Multi-glazing (including double-glazing) windows have attracted increasing attention over the recent years due to their effective performance in saving energy consumption. The common medium between two glass panes is stationary air or inert gas and it could be treated as an extra component in multi-glazing windows. This opens possibilities to apply different fluids and promising filling materials, including airflow, flowing liquid, aerogel and phase change material (PCM), as advanced inter-pane medium to further enhance window performance and match different requirements in different climates. To facilitate the application and further development of such application technologies, this paper aims to provide a comprehensive review mainly including: application technologies, performance assessment methods and indicators, and performance analysis of different application technologies. Also, a comparison of energy saving potentials of different advanced inter-pane mediums in different climates is provided. In addition, the suggestions for future works are given based on current progress.

Keywords: Multi-glazing window; Airflow; flowing liquid; Aerogel; Phase change material

1. Introduction

In recent years, solutions to reduce energy consumption have been paid more and more attention, owing to energy crises. According to [1], building energy consumption account for more than one-third of total energy. A large part of building energy consumption is caused by heat loss through the envelopes (i.e., roof, walls, doors and windows), among which windows are the weakest thermal components [2]. Hence, the window system possesses a great potential to reduce the building energy consumption.

Over the last years, some glazing materials (e.g., tinted glazing) and coatings (e.g., thermochromic coating) have been developed to improve window optical properties [3]. To enhance window thermal properties, an effective way is to multiply the number of glass panes, which is popular in both new buildings and retrofitted historic buildings [4–8]. As reported in [8], by replacing a single pane window with a double pane window, 72.6% energy could be saved in a warm region of Mexico. In the multi-glazing windows, the space between two glass panes is often filled with air or inert gas and it can be treated as an additional component. This opens possibilities to apply airflow, flowing liquid, aerogel and PCM as advanced inter-pane medium to further improve window thermal and energy performances. In the development of application technologies, different types of liquids and promising materials (including aerogels and PCMs), different operation modes of airflow and flowing liquid, and different window structures have been proposed. The thermal and energy performances of the

proposed application technologies as well as the influential factors have been widely investigated in studies. In addition, some attention have been paid on the performance assessment methods especially for the numerical modelling methods as the use of advanced inter-pane medium does add difficulties in describing the heat transfer process in multi-glazing windows. To facilitate the application of advanced inter-pane medium and to further develop application technologies, a comprehensive review including the existing application technologies, performance assessment methods and performance indicators, and performance analysis of different application technologies is required.

The paper is structured into six sections: Section 1 presents the motivation of this review. Section 2 summarizes the application technologies of each advanced inter-pane medium as well as advantages and limitations of each medium in applications. In section 3, experimental and numerical modeling methods as well as performance indicators are introduced. Section 4 reviews comparative studies and parametric studies carried out for investigating performance of different application technologies and compares energy saving potentials of different inter-pane mediums under different climates. Section 5 provides suggestions for future researches and section 6 concludes this paper.

2. Application technologies of advanced inter-pane medium

In this section, application technologies of different advanced inter-pane mediums (i.e., airflow, flowing liquid, aerogel and PCM) are summarized. Also, advantages and disadvantages of each inter-pane medium in real applications are summarized and compared.

2.1 Application of airflow

The air flowing through the cavity between two glass panes could be driven by either natural or mechanical forces. As illustrated in Fig. 1, the ventilation mode can be designed as supply mode, exhaust mode, indoor air curtain mode, outdoor air curtain mode and dual airflow mode [9,10]. In the supply mode, the outdoor fresh air is provided and it is preheated by the solar radiation and the heat escaped from the interior glass before it enters a room. Thus, the supply-air window is often applied in cold climates to function as both a heat reclaim device and a solar collector. Similar to the supply mode, the indoor air curtain mode is also suitable for winter conditions. In the exhaust mode, the indoor air is drawn out through the channel to cool the glass panes and remove accumulated heat in the cavity. Thus, the exhausting airflow window is often treated as a passive cooling system in summer. The airflow window operated in outdoor air curtain mode holds the same function as the exhausting airflow window. In the dual airflow mode, the supply fresh air could be preheated and cooled by the exhaust air in winter and summer, respectively. Thus, the dual-airflow window is suitable for different climates acting like a heat exchanger. Another possible solution to achieve good performance in regions that have both heating demand in winter and cooling demand in summer is using reversible ventilated windows. In the reversible ventilated windows, airflow is operated in indoor air curtain mode under winter conditions and operated in outdoor air curtain mode under summer conditions. It should be mentioned that the inner glass of the double windows illustrated in Fig. 1 could be an insulated double-glazing unit to improve window thermal performance.

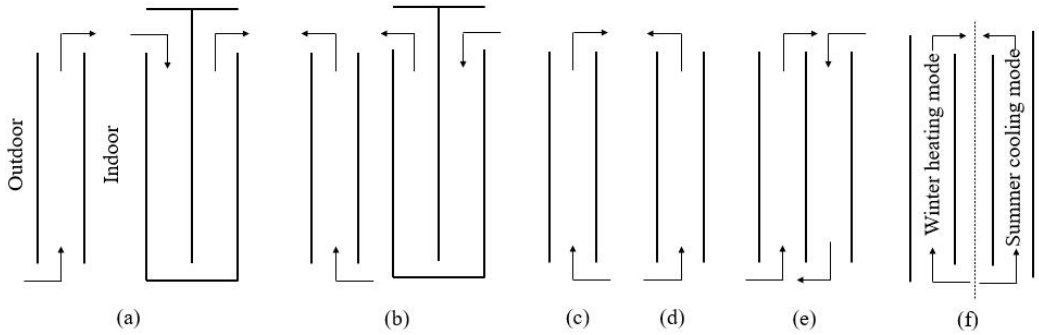

Fig.1. Ventilation modes: (a) supply mode; (b) exhaust mode; (c) indoor air curtain mode; (d) outdoor air curtain mode; (e) dual airflow mode; (f) indoor air curtain mode in winter and outdoor air curtain mode in summer

2.2 Application of flowing liquid

The applied liquids in multi-glazing windows can be divided into three categories: pure water [11], anti-freeze liquid [12] and coloring liquid [13–15]. The application of flowing liquid could improve the window's heat storage behavior and the absorbed heat in liquid could be used to pre-heat the domestic hot water through fluid circulation. The fluid circulation can be designed as closed-loop circulation or open-loop circulation. In the closed-loop system (Fig. 2(a)), the fluid in the cavity between two glass panes keeps circulating inside and it exchanges heat with the feed water through the heat exchanger. To reduce piping requirement, Chow et al. proposed a closed-loop system with a submerged heat exchanger as shown in Fig. 2(b) [16]. In the open-loop circulation (Fig. 2(c)), the feed water is directly supplied into the cavity to absorb solar heat gain and later extracted from the cavity.

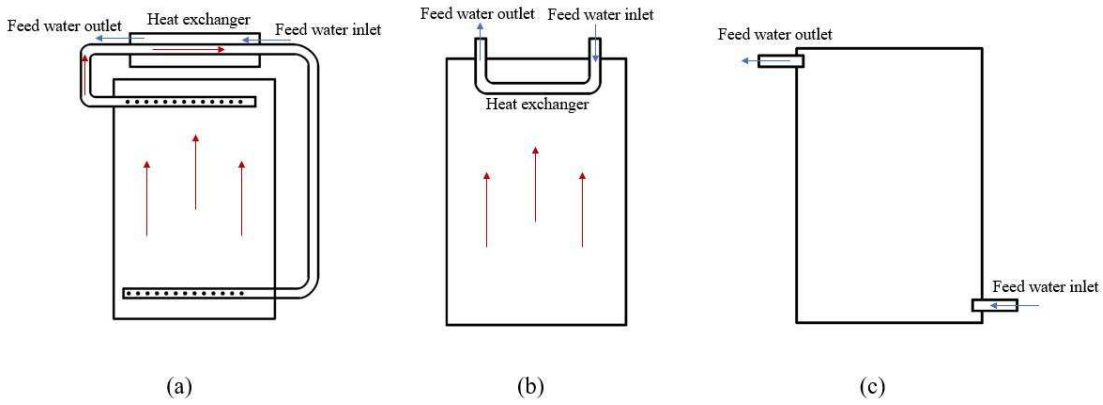

Fig. 2. Fluid circulation: (a) closed-loop circulation; (b) closed-loop circulation with a submerged heat exchanger; (c) open-loop circulation

The simple liquid-flow window configuration is composed of two glass panes and a liquid-flow layer. Due to the fact that the thermal conductivity of liquid is higher than that of air, some configurations made of triple or multiple glass panes (as shown in Fig. 3) have been proposed to integrate liquid-flow layer with some components of low thermal conductivity such as air layer [17], inert gas layer [18] and vacuum gap [19].

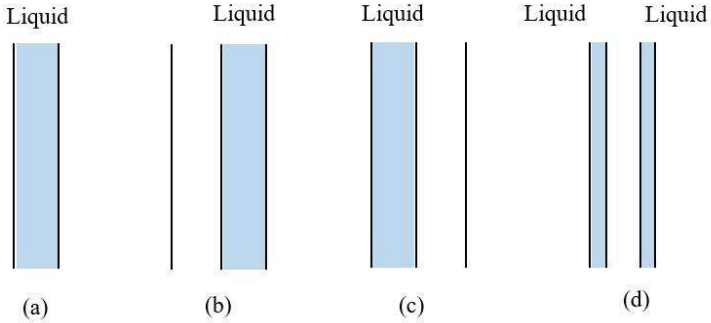

Fig. 3. Configurations of liquid-flow windows

Another characteristic of liquid-flow windows is that the inlet liquid temperature is sometimes controlled at a constant value. According to this, the liquid-flow window could

function as a heating or cooling radiator to achieve desired performances. The control systems and strategies are different from case to case as shown in Table 1.

Table 1 Control systems and strategies of inlet water temperature

Configuration	Control system	Control strategy	Ref.
Glass/ water/ glass;	Electric heater	The inlet temperature is taken as a constant value.	[20,21]
Glass/ argon/ glass/ water/ glass;	Ground source heat exchanger	The inlet temperature is taken as a constant value; Water keeps circulating in summer, and it stays in the cavity until reaching 35 °C in winter.	[22]
Glass/ vacuum gap/ glass/ water/ glass (cooling season); Glass/ water/ glass/ vacuum gap/ glass (heating season);	Not mentioned	Warm water is supplied when there are more than 15 days with daily average temperature lower than 21 °C, and cold water is supplied for the remaining period.	[19]
Glass/ water/ glass/ air/ low-e glass/ water/ glass;	Ground source heat exchanger	For the outer fluid, its inlet temperature is taken as outdoor air temperature; For the inner fluid, its inlet temperature is fixed at 16.7 °C.	[23]
Glass/ water/ glass/ air/ low-e glass/ water/ glass;	Ground source heat exchanger	For the outer fluid, its inlet temperature is taken as outdoor air temperature; For the inner fluid, its inlet temperature is fixed at 22.9 °C.	[24]
Glass/ water/ glass/ air/ glass/ water/ glass;	Not mentioned	For the outer fluid, its inlet temperature is taken as ambient temperature; For the inner fluid, its inlet temperature is fixed at constant value (34 °C, 37 °C and 40 °C) in January, February and December, and it is set as ambient temperature in other months.	[25]

2.3 Application of aerogel

Aerogel is a porous material that has a super lightweight property and a low thermal conductivity. In this view, aerogel is often used in double glazing as an additional insulation

layer. The employed aerogel can be divided into two categories: granular aerogel and monolithic aerogel [26]. Compared to the granular aerogel, the monolithic aerogel shows a better performance in terms of higher light transmittance together with higher insulation performance [27]. Nevertheless, the application of the monolithic aerogel is restricted due to the difficulty in the production of monolithic aerogel with a high optical quality [28].

2.4 Application of PCM

The PCM is a substance which is capable of releasing/absorbing a large amount of energy in the form of latent heat based on phase changing. The phase transition can be classified into four states: solid-solid, solid-liquid, gas-solid and gas-liquid [29]. For practical purpose, only the solid-liquid PCMs can be used for building applications [30]. There is a wide variety of commercial PCMs with different melting temperatures. Commonly, the PCMs are classified into three types: organic (e.g., paraffin, fatty acid), inorganic (e.g., salt hydrates and metals) and eutectic (e.g., capric + lauric acid) [31,32]. Each type of PCM has some advantages and disadvantages for use in buildings, which have been summarized in previous studies [29,30]. The main limitation for most PCMs is the low thermal conductivity which indicates a long time is required to completing the melting or solidification process [32]. This adds the difficulty of PCM applications in buildings. To enhance the thermal conductivity of PCMs, a number of approaches have been proposed such as adding metal structures, microparticles and nanoparticles and impregnating porous material with PCM [30,32,33]. Among these approaches, the addition of nanoparticles has attracted more and more attentions

due to the fact that nanoparticles have super high thermal conductivities and small sizes (less than 100 nm). The nanoparticles could be divided into the following types: carbon-based, ceramic-based, metal-based, polymer-based and semiconductor [33]. The excellent performance of nanoparticles in improving the thermal conductivity of PCMs has been revealed in studies [34,35]. The nano-enhanced PCMs have been applied in some fields to improve energy storage capacity [33,36], but its application in multi-glazing windows is still limited.

The use of PCMs as inter-pane could improve the thermal inertia of windows. The simple prototype of PCM glazing is composed of two clear glass panes and a PCM layer (Fig. 4 (a)). Due to the fact that the PCM has a higher thermal conductivity than air layer, some researchers proposed multi-panes glazing as shown in Fig.4. by filling PCM in the inner or outer cavity [37,38] or integrating the PCM layer with the aerogel layer [39] to achieve a required conductivity. Moreover, the utilization of outer gas layer or aerogel layer could help activate the PCM's melting process in severe cold climate, and the inner gas layer is suitable for hot climate to avoid overheating phenomenon.

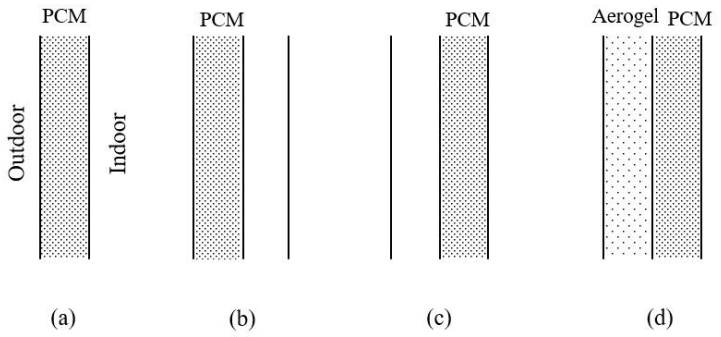

Fig. 4. Configurations of PCM windows

The advantages and disadvantages of each advanced inter-pane medium in real applications are summarized in Table 2.

Table 2 *Comparison of advanced inter-pane medium*

Inter-pane medium	**Advantages**	**Disadvantages**
Airflow	– Light-weight; – Transparent.	– Condensation problem under humid conditions and at low ambient temperature. – Additional fans are needed for mechanical ventilation;
Flowing liquid	– Transparent; – High heat capacity.	– Heavy-weight; – Leakage risk; – Additional facilities are needed such as piping and heat exchanger.
Aerogel	– High insulation performance; – Light-weight.	– Durability issue; – Subsidence problem; – Translucent.
PCM	– High thermal energy storage capacity.	– Translucent in the solid state; – Increased weight; – Leakage problem.

3. Performance assessment methods and indicators

In this section, experimental and numerical methods as well as performance indicators for assessing the feasibility of different application technologies are summarized and discussed.

3.1 Performance assessment methods

3.1.1 Experimental methods

Experiments are necessary to test the actual performance of a given multi-glazing window and validate numerical methods. According to boundary conditions in testing,

experimental methods are divided into two types: laboratory experiments and in-situ experiments.

Laboratory experiments are conducted under controlled conditions to measure steady-state thermal and optical properties. For thermal properties measurements, the guarded hot plate (GHP) method, the heat flow meter (HFM) method and the hot box (HB) method are three standard methods [40–46]. As shown in Fig.5 (a), the GHP apparatus is composed of two cooling units and a heating unit surrounded by guarded sections. Specimens are placed between the cooling and heating unit. In the GHP method, the power supplied to the heating unit is measured to determine the heat flow through the specimen. The HFM apparatus (as shown in Fig.5 (b)) is similar to the GHP apparatus. In the HFM method, the heat flow densities are measured by heat flux meters placed on the surface of the specimen. The HB method includes the guarded hot box (GHB) method and the calibrated hot box (CHB) method. As illustrated in Fig.5 (c) and (d), the GHB apparatus is composed of a guard box, a metering box and a cold box, and the CHB apparatus is composed of a metering box and a cold box. The specimen is placed between the metering box and the cold box. In the HB method, the heat flow through the sample is determined by the energy supplied to the measuring box, the calibrated metering box loss and flanking loss. Among the above methods, the GHP method and HFM method are suited for glass units with homogeneous structures. While for full-scale windows with inhomogeneous structures, the HB method is recommended. For optical properties measurements, they are typically performed for multi-glazing windows filled with translucent materials (i.e., aerogel and PCMs). The commonly

used facilities include spectrometer, spectrophotometer, or spectrophotometer with an integrating sphere. In [47], the authors measured PCM-filled double glazing units based on a commercial spectrometer and a dedicated test bed including a large integrating sphere. In the measurements, the spectral was set in the range of 300–2500 nm to get the spectral data (i.e., spectral transmittance, absorptance and reflectance). They concluded that a dedicated test bed was necessary for scattering and diffusing glazing units, as the commercial spectrophotometer might have difficulties in providing accurate measurement. With the measured spectral data, the solar and visible transmittance could be calculated by following the methods described in the International standard ISO 9050 [48]. Based on the measured window thermal and optical properties, the applicability of advanced inter-pane medium could be deduced. Moreover, attributed to the controllability of laboratory experiments, they are often taken for parametric studies to identify important influential factors and their effects.

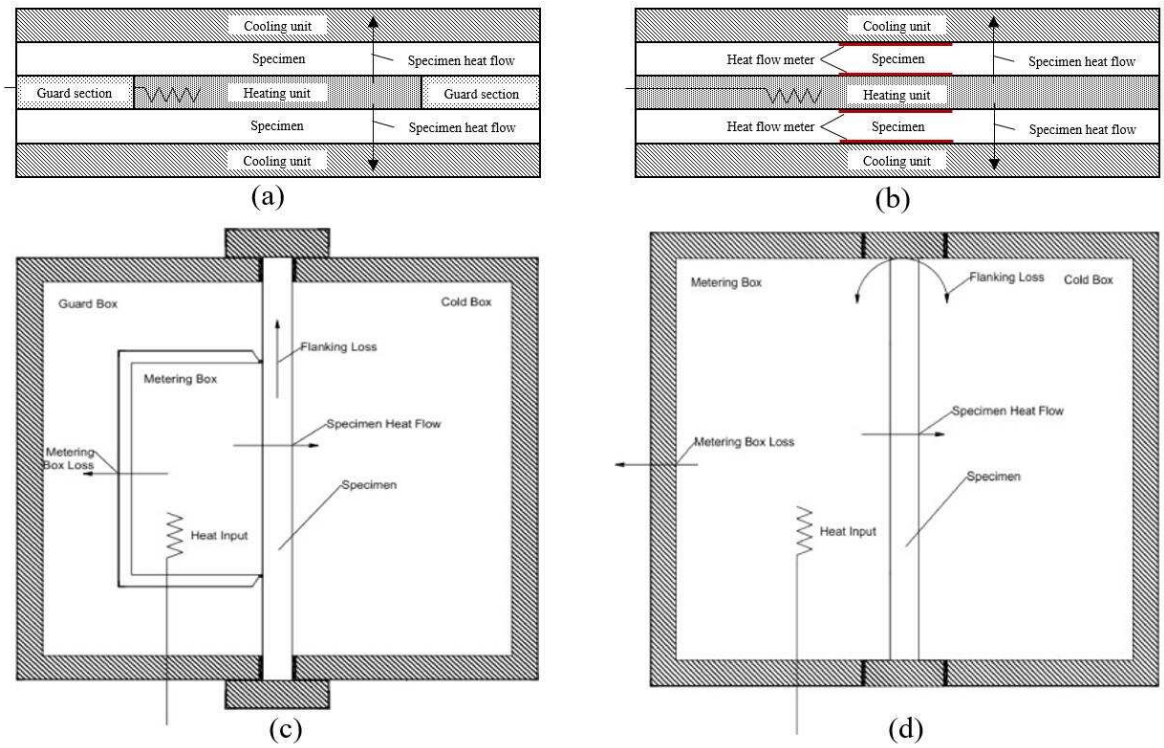

Fig. 5. Laboratory methods: (a) GHP method, (b) HFM method, (c) GHB method [49], (d) CHB method [49]

In-situ experiments are taken under real conditions to test and understand window performance in real applications. The in-situ experiment apparatuses are determined by the purposes of the experiments such as dynamic performance assessment and model validation. The international standard ISO 9869 introduces the in-situ measurement of thermal transmittance by using thermocouples and heat flux meters [50]. In in-situ experiments, several influencing factors simultaneously act during the measurement and it is therefore difficult to take single factor analysis. Nevertheless, in-situ experiments could be carried out for comparative studies with two similar test rooms (as shown in Fig.6) to infer the contributions of the advanced inter-pane medium.

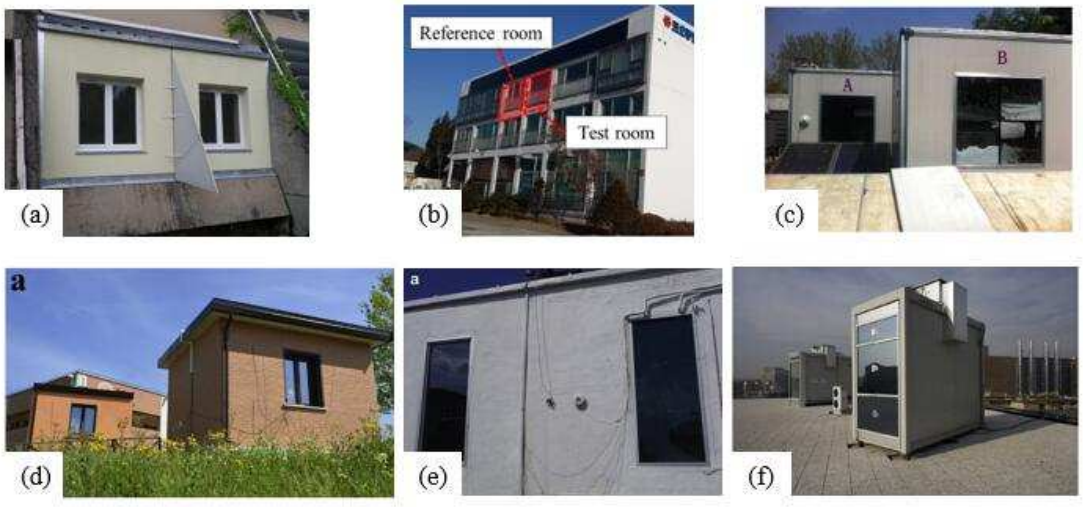

Fig.6. Test-beddings for comparative studies: (a) HYBCELL in Lyon, France [9]; (b) Test rooms in a real building in Gyeonggi-do, Korea [51]; (c) Test cells in Nanjing, China [52]; (d) Test cells in Perugia, Italy [28]; (e) test cells in Hong Kong, China [53]; (f) TWINS test cell facility in Torino, Italy [54];

3.1.2 Numerical methods and treatments

The numerical simulation is a cost-saving and time-saving way to do both comparative studies and parametric studies. The use of airflow, flowing liquid, aerogel and PCM as inter-pane medium in multi-glazing windows adds difficulties in replicating the heat transfer process through numerical simulations. Some of the most complex parts that should be carefully considered in numerical simulations are: the phase change problem, the flow problem and the optical problem. According to this, different numerical models and treatments have been provided, and main equations and hypotheses adopted for models are summarized and discussed in the following.

(1) Numerical treatments on phase change problem

According to the treatments on phase change problem, numerical models are classified into heat capacity methods and enthalpy methods.

- Heat capacity method

In the heat capacity method, the temperature is the only variable. The equations for solid state, liquid state and liquid-solid interface are:

$$\rho_{pcm} c_{pcm,s} \frac{\partial T_{pcm,s}}{\partial \tau} = \frac{\partial^2 T_{pcm,s}}{\partial_x{}^2} + \dot{\Phi}_s \quad ($$

1)

$$\rho_{pcm} c_{pcm,l} \frac{\partial T_{pcm,l}}{\partial \tau} = \frac{\partial^2 T_{pcm,l}}{\partial_x{}^2} + \dot{\Phi}_l \quad (2)$$

$$\lambda_{pcm,s} \frac{\partial T_{pcm,s}}{\partial x} - \lambda_{pcm,l} \frac{\partial T_{pcm,l}}{\partial x} + \dot{\Phi} = \rho_{pcm} H \frac{dS}{d\tau} \quad (3)$$

Where ρ is the density, kg/m^3; c is the specific heat capacity, kJ/kg K; λ is the thermal conductivity, W/m K, H is the specific enthalpy, kJ/kg; $\dot{\Phi}$ is the absorbed heat, W/m^2; S is the position of the liquid-solid interface, and the subscript *s* and *l* represent solid PCMs and liquid PCMs, respectively.

The complicated problem in such numerical analysis is that the solid-liquid boundary moves in the melting or solidification process. To solve this problem, Ismail and Henríquez utilized the moving grid procedure [55]. In the moving grid procedure, the direction of melting/re-solidification is required as a priori. While the real melting/re-solidification process is complex and it does not necessarily occur from one side to another side. Therefore, Goia et al. developed a simplified numerical model which transforms the "multi-phase" problem into a "single-phase" problem by defining an equivalent heat capacity [56]:

$$\rho_{pcm} c^*_{pcm} \frac{\partial T_{pcm}}{\partial t} = \lambda_{pcm} \frac{\partial^2 T_{pcm}}{\partial_x{}^2} + \dot{\Phi} \quad (4)$$

The equivalent heat capacity (c^*_{pcm}) in Eq. (4) was described as a function of temperature. The results showed that the simulated data and measured data on surface temperature were in

close proximity, while there was a deviation between the simulated and measured transmitted radiation and heat fluxes [56].

- Enthalpy method

The enthalpy method is a popular method to solve the phase change problem as it does not require to track the moving boundary [52]. In this method, the specific enthalpy is defined as the variable. The governing equation is expressed as Eq. (5).

$$\rho_{pcm}\frac{\partial H}{\partial \tau} = \lambda_{pcm}\frac{\partial^2 T_{pcm}}{\partial x^2} + \dot{\Phi} \quad (5)$$

The enthalpy in Eq. (5) is the sum of sensible and latent heat of the PCM, that is,

$$H = \int_{T_{pcm,s}}^{T} \rho_{pcm,k} c_{pcm,k} dt + \rho_{pcm}\beta(T)Q_L \quad (6)$$

Where β represents the liquid fraction. The function $\beta(T)$ is typically described by the Eq. (7) based on the linear assumption which may not be really the case [57].

$$\beta(T) = \begin{cases} 0 \ (T < T_{pcm,s}) \\ \dfrac{T - T_{pcm,s}}{T_{pcm,l} - T_{pcm,s}} \ (T_{pcm,s} \le T \le T_{pcm,l}) \\ 1 \ (T > T_{pcm,l}) \end{cases} \quad (7)$$

(2) Numerical treatments on fluid problem

According to the treatments on the fluid problem, the numerical models for fluid medium could be categorized into fluid-simplified models and CFD models.

- Fluid-simplified model

In the fluid-simplified model, the fluid medium between two glass panes is modeled based on either zero-dimension or one-dimension assumption. For the zero-dimension

assumption, the total fluid medium is assumed uniform and for the one-dimension assumption, the fluid medium is divided into several sections along with the height. The heat transfer between fluid medium and glass panes is calculated based on the convective heat transfer coefficient (h_c) which is determined by empirical correlations. The energy balance equation for the one-dimensional model can be written as Eq. (8).

$$\rho c V \frac{\partial T_{f,j}}{\partial \tau} = A_j h_c\left(T_{go,j} - T_{f,j}\right) + A_j h_c\left(T_{gi,j} - T_{f,j}\right) + c\dot{m}\left(T_{f,j} - T_{f,j-1}\right) + \dot{\Phi} \quad (8)$$

Where A is the area of glass surface j, m^2; V is the volume, m^3; $\dot{m}$ is mass flow rate of the fluid, kg/s; $\dot{\Phi}$ is 0 when the fluid is airflow, and the subscript *go*, *gi* and *f* represent the outer glass pane, the inner glass pane and the fluid, respectively.

This simplified model is suitable for long-term simulations and adapted in building energy simulation tools (e.g., EnergyPlus). It should be mentioned that estimation errors may occur if the empirical correlation is not precisely fit for the studied phenomenon.

- Computational fluid dynamic (CFD) model

In the CFD model, the fluid medium is modeled based on two- or three-dimensional assumptions by meshing the fluid region into finite number of control volumes [58,59]. Navier-Stokes equations, mass balance equation and energy balance equation are established for each controlled volume to get detailed temperature and velocity filed. The Navier-Stokes equations for the fluid medium are as Eq. (9) and (10).

$$\frac{\partial u}{\partial \tau} + u\frac{\partial u}{\partial x} + v\frac{\partial u}{\partial y} = -\frac{1}{\rho}\frac{\partial p}{\partial x} + \frac{\mu}{\rho}\left(\frac{\partial^2 u}{\partial_x{}^2} + \frac{\partial^2 u}{\partial_y{}^2}\right) \quad (9)$$

9)

$$\frac{\partial v}{\partial \tau} + u\frac{\partial v}{\partial x} + v\frac{\partial v}{\partial y} = -\frac{1}{\rho}\frac{\partial p}{\partial x} + \frac{\mu}{\rho}\left(\frac{\partial^2 v}{\partial_x{}^2} + \frac{\partial^2 v}{\partial_y{}^2}\right) + g\beta(T - T_\infty) \quad (10)$$

Where u and v are the velocity, m/s; μ is the dynamic viscosity, kg/ms; β is the thermal expansion coefficient, K^{-1}; T_∞ is the temperature in the undisturbed fluid far from the surface, K.

(3) Numerical treatments on the optical problem

According to the complexity of the optical assumption, the numerical method for radiative heat transfer could be classified into the radiosity method and radiative transport equation (RTE) solutions.

- Radiosity method

The radiosity method is based on the following assumption: (1) the glass panes are assumed as grey bodies and opaque to thermal radiation; (2) the inter-pane medium is assumed as a non-participating medium. In the radiosity method (as shown in Eq. (11)), the view factor (F_{ij}) needs to be calculated before simulating the radiation. The view factor is determined by the surfaces' size, separation distance and orientation [40].

$$J_i = \varepsilon_i \sigma T_i^4 + (1 - \varepsilon_i)\sum_{j=1}^{N} F_{ij} J_j \quad (11)$$

Where ε_i is the emissivity of surface i, σ is the Stefan-Boltzmann constant, W/m^2K^4, J_i is the radiosity of surface j, W/m^2.

- Radiative transport equation (RTE) solutions

The radiative transport equation for an absorbing, emitting, scattering medium can be written as [60]

$$\frac{dI_\eta}{ds} = k_\eta I_{b\eta} - k_\eta I_\eta - \sigma_{s\eta} I_\eta + \frac{\sigma_{s\eta}}{4\pi} \int_{\Omega=4\pi} I_\eta(\hat{s}_i) \Phi_\eta(\hat{s}_i, \hat{s}) d\Omega_i \quad (12)$$

Where $\hat{s}_i$, $\hat{s}$ is the direction vector; k is the absorption coefficient, K^{-1}; σ is the absorption coefficient, m^{-1}; Φ is the phase function; Ω is the solid angle; the subscript η represents the wavelength.

In this equation, the radiation intensity and temperature are two variables. The integration of the radiation intensity is the solar source term in the energy balance equation which is written as

$$\int_{\Omega=4\pi} \frac{dI_\eta}{ds} d\Omega_i = \nabla \cdot q_r \quad (15)$$

The discrete ordinates model is commonly used to solve the RTE equation.

3.2 Performance indicators

3.2.1 Thermal and optical property indicators

Thermal transmittance (*U*-value), solar heat gain coefficient (*SHGC*, also called *g*-value) and visible transmittance (*VT*) are three standard indicators implied in many studies for characterizing the thermal and optical properties of windows [61].

The standard *U*-value (W/m^2 K) represents the heat transferred through per m^2 of the given window under one degree of the temperature difference (ΔT) between indoor and outdoor air temperatures. Considering that the heat loss through the interior glass is partly recovered when the supply airflow is applied, the equivalent *U*-value (U_e, W/m^2 K) which represents the heat escaped from per m^2 of the exterior glass under one degree of ΔT was firstly proposed by [62]. A lower *U*-value indicates a higher insulation performance and it should be as low as possible. The *g*-value is the fraction of incident solar radiation that enters into the room, and it is sometimes replaced by the shading coefficient (SC) which is the ratio of the *g*-value for the given window to that of a 3 mm thick clear glass. The favorable *g*-value differs between climates: high one for cold climates and low one for hot climate. The *VT* is the percentage of visible light that transmits through the window. A window with high value of *VT* could provide pleasant view of outside and a good amount of light but it also contributes to high heat gains as well as potential glare.

These indicators can support decision making during design and refurbishment process regardless of the building. Moreover, the *U*-value and *g*-value are widely used in building simulation tools such as EnergyPlus to simulate energy performances. However, these indicators are static and thus they cannot reflect window dynamic performance in real climate conditions.

3.2.2 Energy performance indicators

Energy evaluation of a window is commonly carried out in terms of heat gain/loss, energy demand and energy saving rate. The heat gain/loss (also called energy consumption of

window and total transmitted energy) is an indicator from the aspect of window level. It includes the solar radiation that directly transmits through the window and the convective heat transfer between the interior surface and the indoor air. The energy demand (also called energy consumption and energy load) is an indicator from the aspect of building level. The total energy demand should take that for heating, cooling, lighting, and also for additional facilities such as pump and fans into consideration. Energy saving rate is a measure of relative difference between the energy gained by the given window and the reference window.

For the supply-air window, the heat recovered from the heat loss through the inner glass is an additional indicator to evaluate the window's capability as a heat reclaim device. For the liquid-flow window, the heat gained by the liquid-flow layer is an extra indicator to reveal its capacity to preheat domestic water.

4. Performance analysis of different application technologies

In this section, the comparative studies and parametric studies carried out for identifying performances of different application technologies are summarized. Also, energy saving potentials of each advanced inter-pane medium are compared under different climates.

4.1 Thermal and optical properties

Wright carried out simulations for eleven window configurations composed of different inner and outer glazing, with or without supply air flow [62]. It was found that, the supply air-flow utilization could lead to 31–58% reduction of *U*-value and 1–5% increase of *SC* value. Also, the author noted the low-e coating could better exert its benefit when it was placed on

the surface of the inner glazing that faces the air flow channel. A similar finding was reported in [63] that U_e-value was almost reduced by 50% by changing the position of low-e coating. Another finding in [63] was that an increase of the supply air flow rate from 5.6 l/s to 14 l/s in a 30 mm cavity led to a decrease in U_e-value. Another parametric study with varying air flow rates could be observed in [64] based on a modified guarded hot box. The experimental results showed that the recovered heat gain was increased with increasing the air flow rate, while the heat recovery lost its effect on energy saving when the air flow rate was larger than 6 l/s in an 83 mm air channel. In a later study performed by [65], the correlation between the window aera and U_e-value was calculated based on CFD simulations. Carlos and Corvacho provided U_e-value and *g*-value of supply-air windows with different configurations and different air flow rates [66,67].

Skaff and Gosselin performed CFD simulations and identified *U*-value and *g*-value of a double insulated glazing unit and a ventilated glazing unit operated in exhaust mode or outdoor air curtain mode with varying cavity widths under NFRC design conditions (783 W/m^2 solar radiation, 24 °C indoor temperature and 35 °C outdoor temperature) [68]. The *g*-value of the ventilated glazing unit was lower than that of the insulated glazing unit regardless of operation modes. In addition, *g*-value almost remained the same value as the cavity width increased, which is consistent with the result reported in [69,70]. For the *U*-value, it was decreased when the airflow operated in exhaust mode was applied and but it was increased when the airflow operated in outdoor air circulation mode was applied. A similar finding could be observed in [70] that an increase of air entry temperature led to a deterioration of

window performance. Another interesting finding in [68] was that the *U*-value of the ventilated glazing unit operated in exhaust mode was decreased as the air channel width increased until 3 cm.

A number of laboratory studies have been done to investigate the thermal and optical properties of aerogel glazing [71–75]. The general finding is that, by adding granular or monolithic aerogel in the same thickness cavity instead of air, the *U*-value, *g*-value and *VT* value all decreased. Mover, compared to the granular aerogel glazing, the monolithic aerogel glazing showed better performance with a higher visible transmittance and a lower thermal transmittance [26]. Several parametric studies reported the impact of granular aerogel thicknesses and particle sizes on window thermal and optical properties [27,76–78]. Gao et al. characterized two aerogel glazing units filled with small (size<0.5 mm) and large (size 3–5 mm) granules by using a spectrophotometer and heat flow meters, and found that the unit with smaller granules had lower *U*-value, *g*-value and *VT* value [27]. In [77], 12 pieces of aerogel glazing with varying granular particle sizes and aerogel filling thicknesses were measured by a spectrometer. The measurement results showed that the *SC* and *VT* values had positive correlations with the particle size and negative correlations with the filling thickness. In addition, the filling thickness has a greater influence than the particle size. Moretti et al. found that as the thickness increased from 10 mm to 35 mm, the *U*-value and *g*-value and *VT* decreased [78]. Another interesting finding was that when the aerogel particle changed from large size to small size, the *g*-value decreased from 0.76 to 0.65 while *U*-value almost did not

change. According to this, the larger particle size is more suitable for cold climates to provide larger solar gains.

With regard to liquid-flow windows and PCM windows, only a few studies have been carried out for identifying their thermal and optical properties [17,47,55]. Sierra and Hernández provided analytical expressions of *g*-value and *U*-value for the water-flow window, which demonstrated that these two values could be modified by changing the water flow rate [17]. The optical properties of double-glazed units filled with liquid and solid PCM were measured in [47] based on a commercial spectrophotometer and a dedicated test bed equipped with a 0.75 m integrating sphere. Ismail and Henriquez characterized the *U*-value and *g*-value of PCM-filled double-glazed units with different filling thicknesses [55]. Their experimental measurement indicated that the *g*-value seemed to be unaffected by the increase of the PCM thickness, while the *U*-value decreased with the increase of the PCM thickness. But they did not mention the PCM state. Further studies for identifying optical and thermal properties of liquid-flow windows and PCM windows are still needed.

4.2 Energy performance

4.2.1 Ventilated window

Carlos et al. conducted experiments based on the outdoor test cells built in Portugal and carried out simulations to investigate the effectiveness of supply-air windows in preheating fresh air for different orientations and different climate regions [79,80]. They concluded that the supply-air window could be chosen for any orientation of buildings where pre-heating

fresh air is needed even if there is a lack of solar radiation. They also tested different configurations by changing the inner window from a single glass window to a double glass window [81]. But they did not compare supply air windows with conventional multi-glazing windows. Barakat performed experiments in Ottawa, Canada, to compare a supply-air window with a double-glazed insulated window and a triple-glazed insulated window [82]. The supply-air window is a sealed double-glazed window retrofitted by adding an extra glazing on the outside. The experiment was conducted for four months during the heating season, and the reductions of energy consumption were shown as 25% and 20% compared to the insulated double-glazed window and triple-glazed window, respectively. In [10], a supply-air triple-glazing window was compared with conventional double- and triple-glazed windows, and it performed better than the conventional ones in terms of daily energy balance.

Skaff and Gosselin also investigated the benefits of introducing the airflow operated in outdoor air curtain mode into different double-glazing units under a summer design condition, in terms of total heat gain [68]. The tested double-glazing units adopted different exterior glass panes with different absorption coefficients. Results pointed out that, the reduction of heat gain caused by the airflow was in the range of 6.8%–55%. The seasonal energy performance of a mechanical ventilated exhausting airflow window in a typical evaporatively-cooled space in Shiraz city was presented in [83]. The average heat gain of the studied window was 16.6% less than that of the absorptive-clear double window during cooling season from May to September. The authors also studied the impact of the air cavity thickness and the window aspect ratio on the window performance in the hottest month. They found

that the heat gain increased with the increase of the cavity thickness but decreased with the increase of the aspect ratio. Considering that extra energy consumption of fans will increase when the cavity thickness is decreased, there is a minimum thickness to achieve positive net energy saving and the minimum thickness is lager for higher aspect ratio. Choi et al performed CFD simulations for an exhausting airflow window which was composed of an outer clear single glass pane and an inner double low-e glazing [51]. From their results, the weekly cooling energy was reduced by 9% when the ventilated window was applied instead of a triple glazing with the same glass panes.

In order to evaluate the performance of a dual-airflow window, a modified EnergyPlus program have been developed [84]. On this basis, Wei et al. carried out a comprehensive parametric study and determined an optimum design for the studied dual-airflow window [85]. The optimized dual-airflow window could save 25% energy for cooling and heating in Guangzhou, 28% in Kunming, 29% in Shanghai, 32% in Beijing and 34% in Harbin, as compared to a conventional triple glazing. In this view, the dual-airflow window has greater potential of energy saving in colder climates.

The energy saving potentials of different reversible ventilated windows have been revealed in several studies [86–90]. Based on the PASLINK test cell in Porto, Leal and Maldonado carried out experiments for a reversible ventilated window (named SOLVENT window) with a fixed double glazing and a movable absorptive glazing [86]. The ESP-r based simulations were latter validated and performed to compare the SOLVENT window with a double clear glazing window and a double-glazed solar control window. The energy demand

for heating, cooling and lighting was reduced by 16% and 8% respectively. The performance of a reversible ventilated window made of a fixed float glass and a moveable absorptive glass under the climates of Hong Kong and Beijing is clearly shown in [87,88]. The authors concluded that the reversible mechanism was not necessary in Hong Kong, but it really had significant energy saving advantage in Beijing. As reported in [88], the total heat gain was reduced by 24.9% compared to a double absorptive-clear glazing system for the summer months in Beijing, but it increased by 46.2% for the winter months.

4.2.2 Liquid-flow window

The double-glazed water-flow window has been extensively studied by a research team in Hong Kong [11,12,16,53,91–95]. In [91], the heat gains of a variety of single-glazed and double-glazed windows were simulated under a steady-state summer condition. A clear-clear double-glazed window resulted in 380 W/m^2 heat gain and this value reduced to 314–319 W/m^2 for the clear-clear water-flow window. Under the climate in Hong Kong, the absorptive-clear water-flow window could reduce annual room heat gain by around 32% in comparison with the absorptive-clear double glazing [92]. When clear-reflective water-flow glazing was utilized, indoor heat gain was reduced by 40% and 13% compared to reflective single glazing and reflective-clear double glazing respectively [93]. In addition, 22–35% reductions of cooling loads were found in a large sport center by replacing clear-reflective water-flow glazing with conventional double glazing [11]. The annual performances of an absorptive-absorptive water-filled glazing with a submerged heat exchanger in nine cities of

China were reported in [16]. Results showed that compared to an air-cavity double glazing, the room heat gain was reduced by 10–20% and the net energy savings (heating, cooling and water heating) achieved 916.85–1813.15 MJ/m^2. Also, a variety of influencing factors including the glazing property [53], glazing height-to-width ratio (GHTWR) [94], water circulation design [95], header design [96], water layer thickness [94], supply water flow rate [95], warm water temperature [95] and concentration of propylene glycol in anti-freeze liquid [12] have been studied by the same research team. The main results are as follows:

- As the GHTWR decreased, the room heat gain was reduced but the water heat gain was improved until the GHTWR was around 0.4. With a further decrease of GHTWR, the water heat gain was reduced [94].
- A higher water heat gain but a lower room heat gain could be found in the open-loop system compared with the closed-loop system [95].
- Modifying the opening diameter or distribution of opening on headers has insignificant effects on the indoor heat gain [96].
- As the water layer thickness increased, both the water heat gain and room heat gain decreased [94].
- When the supply water rate increased from 200 ml/min to 400 ml/min, the water heat gain was improved, but no obvious improvement was observed when the rate had a further increase [95].
- Increasing warm water temperature resulted in a greater room heat gain but a lower water heat gain [95].

- The decrease of the water heat gain could be observed by increasing the anti-freeze concentration [12].

The annual energy performance of a double-glazed water-flow window (see details in Table 1) in the continent climate was evaluated by Gile-Lopez and Gimenez-Molin based on simulations [20,21]. The numerical model was validated by experiments taken in a small box in Madrid, Spain. The energy demand for heating and cooling was reduced by 18.26% compared to the air-filled double glazing. But they did not mention whether the energy used to preheat the water was considered.

The performance of triple-glazed liquid-flow windows could be found in [15,19,22,97]. In [22], the performance of a water-flow window (see details in Table 1) was evaluated based on considering cases with and without use of water heat gain. Based on the presented annual simulation results in thirteen cities, this review shows a calculation of energy saving rates caused by the utilization of water flow. The energy saving rates were in the range of -12–80% and -2–82% for cases without and with use of water heat gain, respectively. In their further research, another similar configuration with dynamic control of liquid transparency was proposed and investigated in seven cities [15]. Lyu et al. performed annual simulations for a vacuum-water flow window (see details in Table 1) in three cities of China [19]. Compared to a double-glazed water-flow window, the room heat gain was reduced by around 42% in cooling climate. While for heating climate, the use of vacuum layer reduced not only heat loss but also the excessive room heat gain when the solar radiation or outdoor temperature was high. An experiment study for the same configuration was carried out in cooling season of

Chengdu, China, by comparing to a similar configuration with an outer insulation air gap instead of a vacuum gap [97].

Li et al. performed simulations of an office room equipped with a quadruple-glazed double-circulation flow window (see details in Table 1) for cooling season in Shanghai, China [23]. The simulations were carried out to achieve zero indoor heat gain (case 1) and zero cooling load (case 2) by varying water flow rates. As compared to the base case with a low-e double-glazed window, the net energy savings for air-conditioning system, water-heating device and pump were found as 576–635 MJ for case 1 and 926.1–1223.5 MJ for case 2. A related study for the same configuration (see details in Table 1) in Shenzhen was presented in [24]. The authors analyzed the window performance with different water flow rates and different water shading rates. Another study for a similar window configuration (see details in Table 1) was also performed in Shenzhen, China [25]. Results showed that the net energy savings were 305 kWh, 273 kWh and 238 kWh for the cases with 34 °C, 37 °C and 40 °C inlet water temperature compared to the normal double-glazed window.

Stopper et al. assessed the energy performance of the quintuple-glazed double-circulation flow windows in Munich (Germany) and Dubai (UAE), based on simulations [98]. In the studied window, the inner fluid layer is clear fluid and the outer fluid layer is clear fluid or dyes fluid. The outer fluid and inner fluid are separated by two Kryton layers. By comparing with the solar control glazing, it was found that found the studied window without coloring the outer fluid increased the cooling demand by around 39% in Munich and 25% in

Dubai. While for the widow with coloring the outer fluid, it decreased the cooling demand by around 23% in Munich and 44% in Dubai, when compared to a solar control glazing.

4.2.3 Aerogel glazing

Two cases in Denmark were numerically investigated for assessing the applicability of monolithic aerogel glazing. One is a new built house insulated according to the Danish building code, and the other is a low-energy house insulated according to the passive house standard [72,73]. As concluded by authors, the annual heating demand for the new built house and the low-energy house could decrease by 19% and 34% respectively by replacing argon-filled triple glazing with aerogel glazing. Berardi replaced double glazing with monolithic aerogel glazing in an educational building in Massachusetts (USA) as a retrofit solution [99]. The simulated energy savings were shown around 12%, 14%, 18%, 21% for 40%, 60%, 80% and 100% replacement. Buratti performed EnergyPlus simulations to evaluate the impact of monolithic aerogel glazing on the building energy performance in different cities of Europe [100]. From their given results, energy savings for heating, cooling and lighting could be calculated. The energy saving rates were 3.7–5.6% for Helsinki (Finland), 2.5–4.3% for Turin (Italy), and 3.1–5.5% for Paris (France), -1.6% for Rome (Italy), when compared to low-e double glazing. Wang et al. evaluated the monolithic aerogel glazing performance in different climate areas of China by using eQuest energy simulation program [101]. From their given results, energy savings for cooling and heating could be calculated compared to a

conventional double-glazing window. The energy saving rates were around 14% for Harbin, 10% for Beijing, 9% for Shanghai, 8% for Guangzhou, and 7% for Kunming, respectively.

A comparison between a granular aerogel glazing, a low-e glazing and a conventional single glass was adopted in Hong Kong based on EnergyPlus simulations [102]. From simulations, it was found that the cooling load reduction caused by the aerogel glazing was almost the same as that caused by the low-e glazing. By properly designing aerogel thicknesses and particle sizes in [103], 8.5% and 5.4% of cooling energy saving could be achieved in Hong Kong compared to the conventional double window and double low-e window respectively. To balance the requirements of energy saving and visible transmittance, the authors suggested 12 mm aerogel thickness and 4 mm particle size. Gao et al. numerically investigated the applicability of aerogel glazing in Norway, in terms of total energy demand for heating, cooling and lighting [104]. Results pointed out that, the use of 14 mm granular aerogel in the cavity between two glass panes instead of air could lead to about 21% reduction in total energy demand. When the aerogel thickness increased to 30 mm, the aerogel glazing had a similar performance with triple low-e glazing. Buratti et al. also investigated the performance of granular aerogel glazing in Rome, Paris and Ottawa [105]. The results showed that the heating energy demand reductions were 13% for Ottawa, 24% for Paris and 29% for Rome, and the cooling energy demand reductions were around 21% for Ottawa, 20% for Paris and 18% for Rome, when compared to a conventional double glazing. However, when the aerogel was integrated with low-e glazing, its benefit on reducing cooling demand was negligible. The feasibility of granular aerogel glazing in four cities (i.e., Harbin, Beijing,

Changsha, Kunming) in China was assessed in [106] by comparing to conventional double glazing, triple glazing and low-e double glazing. Results showed that the aerogel glazing performed better than the other three in heating season, but in cooling season the low-e double glazing was the most suitable one. To improve aerogel glazing performance in warm and hot regions, Belloni et al. proposed a double-glazing unit filled with a mixture of silica granular aerogel and hollow silica powder [107]. They simulated energy demand of an office building in Tokyo with different window orientations, based on EnergyPlus software. A reduction (14–24%) of the cooling demand could be observed attributed to the addition of powder. Moreover, the proposed aerogel glazing outperformed the low-e glazing with 22% (North)–62% (south) reduction of heating energy demand.

4.2.4 PCM glazing

The energy performances of double-glazed PCM windows have been evaluated by several researchers in different climate regions [52,54,108–114]. Goia et al. compared a double-glazed unit filled with RT35 paraffin and a traditional double-glazed unit by taking experiments in the outdoor test cell (TWINS test facility) located in Torino [54,108]. The comparative analyses showed that the PCM-filled unit performed effectively in summer with 20%–55% reduction of daily entering energy, while its performance in mid-season and winter was not as favorable as that in summer. In [52], in-situ experiments were conducted in Nanjing (China) based on two identical outdoor chambers installed with a PCM window and a hollow glass window respectively. With experiment data, the numerical model was validated

and simulations were then performed based on selected typical days. The simulated energy saving rates were found as 39.5%, -43.5%, -78.9% and -5.8% for the sunny summer day, the rainy summer day, the sunny winter day and the rainy winter day, respectively. A similar performance was reported in a study performed in Changsha, another city of China with hot summer and cold winter [113]. Further investigations of the PCM window in Nanjing were carried out by [109] with varying the latent heat of fusion, the melting temperature and the difference between liquidus temperature and solidus temperature. A higher energy saving rate was observed when the latent heat of fusion increased from 205 kJ/kg to 287kJ/kg. In relation to three melting temperature ranges, the energy saving rate was decreased from 18.3% to 8.5% and 10.5% when the melting temperature of 27–29 °C altered to 31–33 °C and 23–25 °C, respectively. In this view, the authors suggested the melting temperature of 25 °C–31 °C for summer conditions in Nanjing. A similar trend of energy saving rate could be observed in varying the temperature differentials between liquidus temperature and solidus temperature of PCM. Liu et al. conducted experiments in the small-scale test facility located in Daqing (China) in two sunny days in October [112]. Based on the measured data, the numerical model was validated to simulate the PCM glazing performance with different melting temperatures (14–16 °C, 16–18 °C and 18–20 °C) and different PCM filling thicknesses (4–50 mm) in a typical summer day. The authors found that, the total transmitted energy decreased by 109.1% as the PCM thickness increased from 4 mm to 50 mm when the melting temperature was 14–16 °C. But the trend of total transmitted energy was not always consistent with the increase in PCM thickness. Increasing the thickness may lead to a reversed

trend for some PCMs. This result is in agreement with [114] in which the total transmitted energy was effectively reduced with increasing the PCM thickness from 4 mm to 30 mm, but the trend was reversed when the thickness was further increased to 50 mm. More comprehensive parametric studies based on a typical summer day in Daqing could be found in [110,111].

There are few studies carried out for learning the application performance of nano-enhanced PCM. Li et al. investigated nano-PCM double-glazing units based on simulations. They selected representative days in summer, autumn and winter in Daqing city to perform simulations to test four different combinations of nanoparticle enhanced PCM considering nanoparticle volume fractions which are 1% and 10% and nanoparticle diameters which are 10 nm and 100 nm [115]. It was found that the heat gain was larger for higher volume fraction, but the influence of the nanoparticle diameter on the heat gain was opposite. Another interesting finding is that the magnitude of impact of the studied parameters is dependent on the season and the highest one is in winter. In their another study [57], the impact of different nanoparticle types (i.e., Cu, CuO and Al_2O_3), volume fractions (i.e., 0.1–10%) and sizes of nanoparticles (i.e., 5–25 nm) on window performance in summer conditions was investigated. They recommended CuO nanoparticles with the size under 15 nm and the volume fraction below 1%.

Assessments of triple-glazed PCM windows are reported in [37,39,116,117]. Li et al. also carried out experiments for a triple glazing filled with PCM in the outer cavity (TW+PCM) in summer days. In the sunny summer day, the heat gain was reduced by 16.6%

and 28% and in the rainy summer day, it was reduced by 14.7% and increased by 4.5%, as compared to the PCM double window (DW+PCM) and the conventional triple glazing (TW) respectively. A similar triple-glazed configuration with an inner argon insulation layer was investigated in summer conditions of Lodz city based on ESP-r software [116]. The simulated results showed that the cooling energy saved by the PCM window were 14.7–25% for east orientation and 11.2–17.1% for west orientation , when compared to a traditional window. Li et al. proposed a triple-glazed aerogel-PCM window and they numerically analyzed the influence of thermal conductivity, density, specific heat and thickness of silica aerogel on the window energy performance in the severe cold climate of China [39]. Among the studied parameters, the thermal conductivity and thickness were the two most important factors. As expected, the lowest energy consumption was found when the thermal conductivity was the lowest and the aerogel thickness was the largest. While there was no latent heat of PCM exploited when the aerogel had large thickness such as 40 mm and 50 mm. In this view, the 30 mm aerogel was recommended for the studied climate condition. Further comparative and parametric studies were recently conducted by [117]. Ten different glazing configurations were proposed: double-glazed window (DW), double-glazed PCM window (DW-Par), double-glazed aerogel window (DW-Sil), triple-glazed window (TW), triple-glazed window with inner PCM layer (TW-Par), triple-glazed window with outer aerogel layer (TW-Sil), triple-glazed aerogel-PCM window (TW-Sil-Par), and three improved TW-Sil-Par for optimization purpose. It was found that applying PCM in either double or triple glazing, the energy consumption was improved due to the fact that PCM layer has lower conductivity than

air layer with the same thickness. In addition, compared to DW, the energy saving was 11.41% for TW-Par and 16.35% for TW-Sil-Par. With a further optimization of TW-Sil-Par, the energy saving rate could achieve 70.16% compared to the DW.

4.3 A comparison of energy saving potentials in different climates

In this section, the reported seasonal and annual energy savings for cooling and heating caused by the utilization of advanced inter-pane medium instead of air layer are summarized in Fig.7.

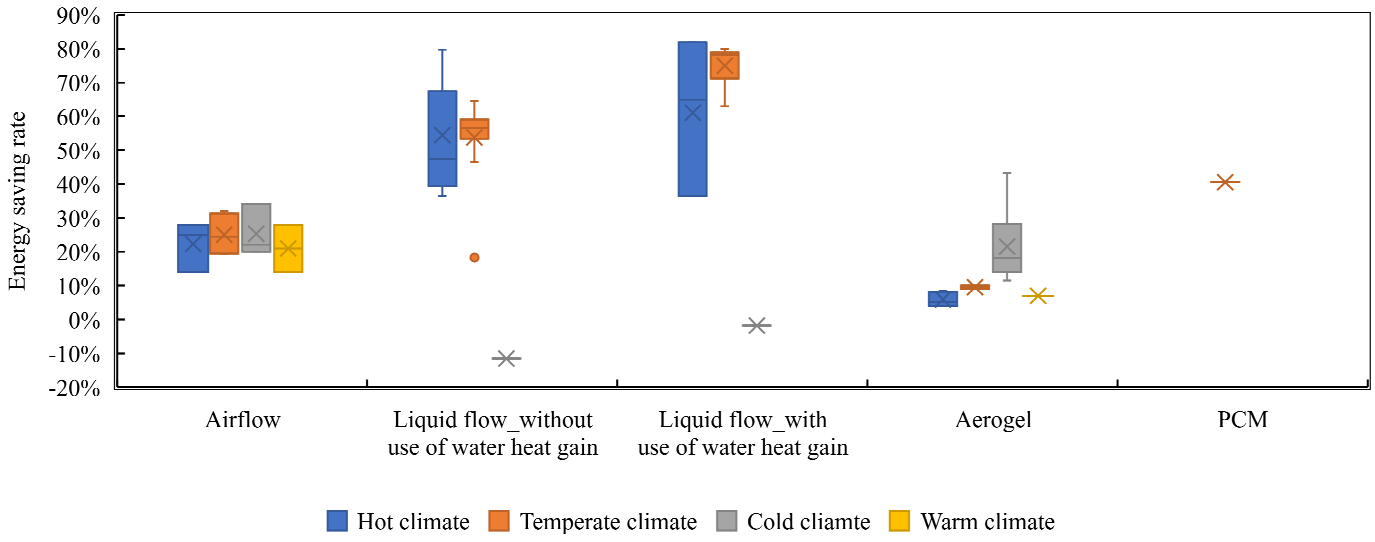

Fig. 7. Energy saving potential of airflow [82,85], flowing liquid [15,20–22], aerogel [28,99,103,105,118] and PCM [52] in different climates

As shown in Fig.7., the average energy saving rates caused by the application of airflow are 22% for hot climate, 25% for temperate climate, 25% for cold climate and 21% for warm

climate. In terms of flowing liquid, the average values are 54% and 61% for hot climate, 54% and 75% for temperate climate and -12% and -2% for cold climate, with and without use of water heat gain respectively. This indicates the application of flowing liquid is more suitable for hot climate and temperate climate rather than the cold climate. In terms of aerogel, the average values are 6% for hot climate, 7% for warm climate, 10% for temperate climate, and 22% for cold climate. In this view, the application of aerogel is more suitable for heating conditions than cooling conditions. In terms of PCM, the value is 41% in Nanjing. Future studies for investigating year-round energy performances of PCM application in different climates are required. Moreover, by comparing the average energy saving rates of different inter-pane mediums under the same climate, it could be concluded that the flowing liquid, airflow, flowing liquid and aerogel have the largest energy saving potential in hot climate, warm climate, temperate climate and cold climate, respectively.

5. Suggestions for future work

A number of researches have been carried out and achieved great progress on the application of advanced inter-pane mediums in multi-glazing windows. To further develop such technologies, some suggestions for future work will be given in this section. First, there are still limited studies focusing on advanced materials such as monolithic aerogel and nano-enhanced PCM which may provide large saving energy potentials. Further explorations are required to investigate the performances and influencing parameters of multi-glazing windows filled with advanced materials. Second, numerous parametric studies have been

conducted based on laboratory experiments and simulation methods to identify the important influencing factors and investigate their effect on window performances. On this basis, some researchers gave optimum values for one or two parameters which are typical local optimizations. While there are far less global optimization studies by considering multiple parameters at the same time. Considering that the global optimization studies are typically time-consuming, a possible effective solution is to perform optimization studies based on simulations and improve simulation efficiency by establishing a numerical model with non-uniform time steps. The non-uniform time steps could be further determined by analyzing the effect of variations of outdoor environments (i.e., outdoor temperature and solar radiation) on window performances. Third, there are few researches considering the effect of applying of advanced inter-pane medium on lighting energy demand which is an important part of energy consumption. Comprehensive building energy simulations are needed in future work especially for the case where the semi-transparent inter-pane medium is employed.

6. Conclusions

Adoption of fluid and promising material as advanced inter-pane medium is an effective method to enhance thermal and energy performance of multi-glazing windows. Various application technologies have been proposed to better exploit benefits of different inter-pane mediums. To investigate the effectiveness of different application technologies and identify the effect of corresponding influential factors, a number of comparative and parametric

studies have been carried out based on experimental or numerical methods. Some main findings are as follows:

(1) The ventilation operation modes, window structures, air flow rates and glazing properties are important parameters which need to be considered in the application of airflow in multi-glazing windows. Attributed to various operation modes, the utilization of airflow could satisfy requirements in different climates.

(2) The benefits of flowing liquid could be better exerted by optimizing window structures, glazing properties and operation parameters (i.e., liquid circulation mode, liquid flow rate, inlet liquid temperature and liquid transparency). The application of flowing liquid is more suitable for hot climate and temperate climate rather than cold climate. There is still a lack of studies for identifying optical and thermal properties of liquid-flow windows.

(3) The aerogel thickness and particle size are two important factors that need to be considered in designing granular aerogel glazing. For the monolithic aerogel glazing, the studies carried out for investigating its influential factors are still lacking. The utilization of aerogel has a great energy saving potential under cold climate but its performance is limited under hot climate. Mixing aerogel with power is a feasible way to improve its performance in hot climate.

(4) The feasibility of applying PCM in multi-glazing windows is highly related with window structures, PCM filling thickness and PCM properties (e.g., conductivity, melting temperature and latent heat). The studies on PCM glazing are mainly conducted in typical days, while there are few studies to assess its seasonal or annual performance to reveal its applicability

under different climates and determine optimum designs. In addition, the application of nano-enhanced PCM in multi-glazing windows still need further explorations.

Acknowledgements

The authors would like to thank the CSC (China Scholarship Council) to provide financial support for the study in France.

References

[1] H. Yoshino, T. Hong, N. Nord, IEA EBC annex 53: Total energy use in buildings—Analysis and evaluation methods, Energy and Buildings. 152 (2017) 124–136. https://doi.org/10.1016/j.enbuild.2017.07.038.

[2] R.Z. Freire, W. Mazuroski, M.O. Abadie, N. Mendes, Capacitive effect on the heat transfer through building glazing systems, Applied Energy. 88 (2011) 4310–4319. https://doi.org/10.1016/j.apenergy.2011.04.006.

[3] M. Aburas, V. Soebarto, T. Williamson, R. Liang, H. Ebendorff-Heidepriem, Y. Wu, Thermochromic smart window technologies for building application: A review, Applied Energy. 255 (2019) 113522. https://doi.org/10.1016/j.apenergy.2019.113522.

[4] M. Coillot, M. el Mankibi, R. Cantin, Heating, ventilating and cooling impacts of double windows on historic buildings in Mediterranean area, Energy Procedia. 133 (2017) 28–41. https://doi.org/10.1016/j.egypro.2017.09.367.

[5] S. Somasundaram, S.R. Thangavelu, A. Chong, Improving building efficiency using low-e coating based retrofit double glazing with solar films, Applied Thermal Engineering. 171 (2020). https://doi.org/10.1016/j.applthermaleng.2020.115064.

[6] S. Somasundaram, A. Chong, Z. Wei, S.R. Thangavelu, Energy saving potential of low-e coating based retrofit double glazing for tropical climate, Energy and Buildings. 206 (2020) 109570. https://doi.org/10.1016/j.enbuild.2019.109570.

[7] M. el Mankibi, R. Cantin, A. Zoubir, Contribution to the thermal renovation of old buildings: Numerical and Experimental approach for characterizing a double window., Energy Procedia. 78 (2015) 2470–2475. https://doi.org/10.1016/j.egypro.2015.11.231.

[8] E. González-Julián, J. Xamán, N.O. Moraga, Y. Chávez, I. Zavala-Guillén, E. Simá, Annual thermal evaluation of a double pane window using glazing available in the Mexican market, Applied Thermal Engineering. 143 (2018) 100–111. https://doi.org/10.1016/j.applthermaleng.2018.07.053.

[9] M. Coillot, Caractérisations numérique et expérimentale du comportement thermo-aéraulique d'une double-fenêtre active, Doctoral Dissertation,Université de Lyon. (2019).

[10] G. Michaux, R. Greffet, P. Salagnac, J. Ridoret, Modelling of an airflow window and numerical investigation of its thermal performances by comparison to conventional double and triple-glazed windows, Applied Energy. 242 (2019) 27–45. https://doi.org/10.1016/j.apenergy.2019.03.029.

[11] T. Chow, C. Li, J.A. Clarke, Numerical prediction of water-flow glazing performance with reflective coating, Proceedings of Building Simulation 2011: 12th Conference of International Building Performance Simulation Association. (2011) 1127–1133.

[12] Y. Lyu, T. Chow, J. Wang, Numerical prediction of thermal performance of liquid-flow window in different climates with anti-freeze, Energy. 157 (2018) 412–423. https://doi.org/10.1016/j.energy.2018.05.140.

[13] D. Gstoehl, J. Stopper, S. Bertsch, D. Schwarz, Fluidised glass façade elements for an active energy transmission control, World Engineers' Convention. (2011).

[14] L. Baumgärtner, R.A. Krasovsky, J. Stopper, J. von Grabe, Evaluation of a solar thermal glass façade with adjustable transparency in cold and hot climates, Energy Procedia. 122 (2017) 211–216. https://doi.org/10.1016/j.egypro.2017.07.347.

[15] M. Gutai, A.G. Kheybari, Energy consumption of hybrid smart water-filled glass (SWFG) building envelope, Energy and Buildings. 230 (2021) 110508. https://doi.org/10.1016/j.enbuild.2020.110508.

[16] T. Chow, W. Liu, Warm climate performance of water-filled double-glazing with submerged heat exchanger, Sustainable Cities and Society. 58 (2020) 102135. https://doi.org/10.1016/j.scs.2020.102135.

[17] P. Sierra, J.A. Hernández, Solar heat gain coefficient of water flow glazings, Energy and Buildings. 139 (2017) 133–145. https://doi.org/10.1016/j.enbuild.2017.01.032.

[18] B.M. Santamaria, F. del A. Gonzalo, B.L. Aguirregabiria, J.A. Hernandez Ramos, Experimental validation of water flow glazing: Transient response in real test rooms, Sustainability (Switzerland). 12 (2020) 1–23. https://doi.org/10.3390/su12145734.

[19] Y. Lyu, W. Liu, H. Su, X. Wu, Numerical analysis on the advantages of evacuated gap insulation of vacuum-water flow window in building energy saving under various climates, Energy. 175 (2019) 353–364. https://doi.org/10.1016/j.energy.2019.03.101.

[20] T. Gil-Lopez, C. Gimenez-Molina, Influence of double glazing with a circulating water chamber on the thermal energy savings in buildings, Energy and Buildings. 56 (2013) 56–65. https://doi.org/10.1016/j.enbuild.2012.10.008.

[21] T. Gil-Lopez, C. Gimenez-Molina, Environmental, economic and energy analysis of double glazing with a circulating water chamber in residential buildings, Applied Energy. 101 (2013) 572–581. https://doi.org/10.1016/j.apenergy.2012.06.055.

[22] M. Gutai, A.G. Kheybari, Energy consumption of water-filled glass (WFG) hybrid building envelope, Energy and Buildings. 218 (2020) 110050. https://doi.org/10.1016/j.enbuild.2020.110050.

[23] C. Li, Y. Lyu, C. Li, Z. Qiu, Energy performance of water flow window as solar collector and cooling terminal under adaptive control, Sustainable Cities and Society. 59 (2020) 102152. https://doi.org/10.1016/j.scs.2020.102152.

[24] C. Li, H. Tang, Evaluation on year-round performance of double-circulation water-flow window, Renewable Energy. 150 (2020) 176–190. https://doi.org/10.1016/j.renene.2019.12.153.

[25] C. Li, C. Li, Y. Lyu, Z. Qiu, Performance of double-circulation water-flow window system as solar collector and indoor heating terminal, Building Simulation. 13 (2020) 575–584. https://doi.org/10.1007/s12273-019-0600-y.

[26] C. Buratti, E. Belloni, F. Merli, M. Zinzi, Aerogel glazing systems for building applications: A review, Energy and Buildings. 231 (2021) 110587. https://doi.org/10.1016/j.enbuild.2020.110587.

[27] T. Gao, B.P. Jelle, T. Ihara, A. Gustavsen, Insulating glazing units with silica aerogel granules: The impact of particle size, Applied Energy. 128 (2014) 27–34. https://doi.org/10.1016/j.apenergy.2014.04.037.

[28] F. Cotana, A.L. Pisello, E. Moretti, C. Buratti, Multipurpose characterization of glazing systems with silica aerogel: In-field experimental analysis of thermal-energy, lighting and acoustic performance, Building and Environment. 81 (2014) 92–102. https://doi.org/10.1016/j.buildenv.2014.06.014.

[29] R. Zeinelabdein, S. Omer, G. Gan, Critical review of latent heat storage systems for free cooling in buildings, Renewable and Sustainable Energy Reviews. 82 (2018) 2843–2868. https://doi.org/10.1016/j.rser.2017.10.046.

[30] H. Akeiber, P. Nejat, M.Z.A. Majid, M.A. Wahid, F. Jomehzadeh, I. Zeynali Famileh, J.K. Calautit, B.R. Hughes, S.A. Zaki, A review on phase change material (PCM) for sustainable passive cooling in building envelopes, Renewable and Sustainable Energy Reviews. 60 (2016) 1470–1497. https://doi.org/10.1016/j.rser.2016.03.036.

[31] D. Li, Y. Wu, B. Wang, C. Liu, M. Arıcı, Optical and thermal performance of glazing units containing PCM in buildings: A review, Construction and Building Materials. 233 (2020) 117327. https://doi.org/10.1016/j.conbuildmat.2019.117327.

[32] Z. Liu, Z. (Jerry) Yu, T. Yang, D. Qin, S. Li, G. Zhang, F. Haghighat, M.M. Joybari, A review on macro-encapsulated phase change material for building envelope applications, Building and Environment. 144 (2018) 281–294. https://doi.org/10.1016/j.buildenv.2018.08.030.

[33] L. Yang, J. nan Huang, F. Zhou, Thermophysical properties and applications of nano-enhanced PCMs: An update review, Energy Conversion and Management. 214 (2020) 112876. https://doi.org/10.1016/j.enconman.2020.112876.

[34] P. Sivasamy, S. Harikrishnan, S.I. Hussain, S. Kalaiselvam, L.G. Babu, Improved thermal characteristics of Ag nanoparticles dispersed myristic acid as composite for low temperature thermal energy storage, Materials Research Express. 6 (2019). https://doi.org/10.1088/2053-1591/ab20ba.

[35] S. Harikrishnan, A. Devaraju, P. Sivasamy, S. Kalaiselvam, Experimental investigation of improved thermal Characteristics of SiO 2 /myristic acid nanofluid as phase change material (PCM), Materials Today: Proceedings. 9 (2019) 397–409. https://doi.org/10.1016/j.matpr.2019.02.169.

[36] S. Harikrishnan, A.D. Dhass, Nanomaterials for Latent Thermal Energy Storage, Handbook of Nanomaterials and Nanocomposites for Energy and Environmental Applications. (2021) 2661–2679. https://doi.org/10.1007/978-3-030-36268-3_97.

[37] S. Li, G. Sun, K. Zou, X. Zhang, Experimental research on the dynamic thermal performance of a novel triple-pane building window filled with PCM, Sustainable Cities and Society. 27 (2016) 15–22. https://doi.org/10.1016/j.scs.2016.08.014.

[38] A. Wieprzkowicz, D. Heim, Thermal performance of PCM-glazing unit under moderate climatic conditions, 7th International Buildings Physics Conference, IBPC2018. (2018) 6.

[39] D. Li, C. Zhang, Q. Li, C. Liu, M. Arıcı, Y. Wu, Thermal performance evaluation of glass window combining silica aerogels and phase change materials for cold climate of China, Applied Thermal Engineering. 165 (2020) 114547. https://doi.org/10.1016/j.applthermaleng.2019.114547.

[40] Y. Sun, Y. Wu, R. Wilson, A review of thermal and optical characterisation of complex window systems and their building performance prediction, Applied Energy. 222 (2018) 729–747. https://doi.org/10.1016/j.apenergy.2018.03.144.

[41] International Standard, ISO 8990: Thermal insulation - determination of steady-state thermal transmission properties - calibrated and guarded hot box, (1994).

[42] International Standard, ISO 8302: Thermal insulation - Determination of steady-state thermal resistance and related properties - Guarded hot plate apparatus, (1991).

[43] International Standard, ISO 8301: Thermal insulation - Determination of steady-state thermal resistance and related properties - Heat flow meter apparatus, (1991).

[44] International Standard, ISO 10291: Glass in building - Determination of steady-state U values (thermal transmittance) of multiple glazing - Guarded hot plate method, (1994).

[45] International Standard, ISO 10293: Glass in building - Determination of steady-state U values (thermal transmittance) of multiple glazing - Heat flow meter method, (1997).

[46] International Standard, ISO 12567-1: Thermal performance of windows and doors - Determination of thermal transmittance by the hot-box method - Part 1: Complete windows and doors, (2010).

[47] F. Goia, M. Zinzi, E. Carnielo, V. Serra, Spectral and angular solar properties of a PCM-filled double glazing unit, Energy and Buildings. 87 (2015) 302–312. https://doi.org/10.1016/j.enbuild.2014.11.019.

[48] I. Standard, ISO 9050:2003, Glass in building - Determination of light transmittance, solar direct transmittance, total solar energy transmittance, ultraviolet transmittance and related glazing factors, (2003).

[49] N. Soares, C. Martins, M. Gonçalves, P. Santos, L.S. da Silva, J.J. Costa, Laboratory and in-situ non-destructive methods to evaluate the thermal transmittance and behavior of walls, windows, and construction elements with innovative materials: A review, Energy and Buildings. 182 (2019) 88–110. https://doi.org/10.1016/j.enbuild.2018.10.021.

[50] International Standard, ISO 9869-1: Thermal insulation - Building elements - In-situ measurement of thermal resistance and thermal transmittance - Part 1: Heat flow meter method, (2014).

[51] H. Choi, Y. An, K. Kang, S. Yoon, T. Kim, Cooling energy performance and thermal characteristics of a naturally ventilated slim double-skin window, Applied Thermal

Engineering. 160 (2019) 114113. https://doi.org/10.1016/j.applthermaleng.2019.114113.

[52] S. Li, K. Zhong, Y. Zhou, X. Zhang, Comparative study on the dynamic heat transfer characteristics of PCM-filled glass window and hollow glass window, Energy and Buildings. 85 (2014) 483–492. https://doi.org/10.1016/j.enbuild.2014.09.054.

[53] T. Chow, C. Li, Liquid-filled solar glazing design for buoyant water-flow, Building and Environment. 60 (2013) 45–55. https://doi.org/10.1016/j.buildenv.2012.11.010.

[54] F. Goia, M. Perino, V. Serra, Experimental analysis of the energy performance of a full-scale PCM glazing prototype, Solar Energy. 100 (2014) 217–233. https://doi.org/10.1016/j.solener.2013.12.002.

[55] K.A.R. Ismail, J.R. Henriquez, Parametric study on composite and PCM glass systems, Energy Conversion and Management. 43 (2002) 973–993. https://doi.org/10.1016/S0196-8904(01)00083-8.

[56] F. Goia, M. Perino, M. Haase, A numerical model to evaluate the thermal behaviour of PCM glazing system configurations, Energy and Buildings. 54 (2012) 141–153. https://doi.org/10.1016/j.enbuild.2012.07.036.

[57] D. Li, Y. Wu, C. Liu, G. Zhang, M. Arıcı, Numerical investigation of thermal and optical performance of window units filled with nanoparticle enhanced PCM, International Journal of Heat and Mass Transfer. 125 (2018) 1321–1332. https://doi.org/10.1016/j.ijheatmasstransfer.2018.04.152.

[58] J.R. Gosselin, Q. Chen, A computational method for calculating heat transfer and airflow through a dual-airflow window, Energy and Buildings. 40 (2008) 452–458. https://doi.org/10.1016/j.enbuild.2007.03.010.

[59] M. Bhamjee, A. Nurick, D.M. Madyira, An experimentally validated mathematical and CFD model of a supply air window: Forced and natural flow, Energy and Buildings. 57 (2013) 289–301. https://doi.org/10.1016/j.enbuild.2012.10.043.

[60] M.F. Modest, Radiative heat transfer, Academic press, 2013.

[61] International Standard, ISO 15099: Thermal performance of windows, doors and shading devices – Detailed calculations, (2003).

[62] J.L. Wright, Effective U-values and shading coefficients of preheat/supply air glazing systems, Solar Energy Society of Canada. (1986) 219–224.

[63] M. Mcevoy, R.G. Southall, P.H. Baker, Test cell evaluation of supply air windows to characterise their optimum performance and its verification by the use of modelling techniques, Energy and Buildings. 35 (2003) 1009–1020. https://doi.org/10.1016/S0378-7788(03)00042-2.

[64] D. Appelfeld, S. Svendsen, Experimental analysis of energy performance of a ventilated window for heat recovery under controlled conditions, Energy and Buildings. 43 (2011) 3200–3207. https://doi.org/10.1016/j.enbuild.2011.08.018.

[65] R.G. Southall, M. Mcevoy, Investigations into the functioning of a supply air window in relation to solar energy as determined by experiment and simulation, Solar Energy. 80 (2006) 512–523. https://doi.org/10.1016/j.solener.2005.04.016.

[66] J.S. Carlos, H. Corvacho, Evaluation of the performance indices of a ventilated double window through experimental and analytical procedures: SHGC-values, Energy and Buildings. 86 (2015) 886–897. https://doi.org/10.1016/j.enbuild.2014.11.002.

[67] J.S. Carlos, H. Corvacho, Evaluation of the performance indices of a ventilated double window through experimental and analytical procedures: Uw-values, Energy and Buildings. 86 (2015) 886–897. https://doi.org/10.1016/j.enbuild.2014.11.002.

[68] M.C. Skaff, L. Gosselin, Summer performance of ventilated windows with absorbing or smart glazings, Solar Energy. 105 (2014) 2–13. https://doi.org/10.1016/j.solener.2013.08.025.

[69] K.A.R. Ismail, J.R. Henriquez, Two-dimensional model for the double glass naturally ventilated window, International Journal of Heat and Mass Transfer. 48 (2005) 461–475. https://doi.org/10.1016/j.ijheatmasstransfer.2004.09.022.

[70] K.A.R. Ismail, J.R. Henriquez, Simplified model for a ventilated glass window under forced air flow conditions, Applied Thermal Engineering. 26 (2006) 295–302. https://doi.org/10.1016/j.applthermaleng.2005.04.023.

[71] K.I. Jensen, J.M. Schultz, F.H. Kristiansen, Development of windows based on highly insulating aerogel glazings, Journal of Non-Crystalline Solids. 350 (2004) 351–357. https://doi.org/10.1016/j.jnoncrysol.2004.06.047.

[72] J.M. Schultz, K.I. Jensen, F.H. Kristiansen, Super insulating aerogel glazing, Solar Energy Materials and Solar Cells. 89 (2005) 275–285. https://doi.org/10.1016/j.solmat.2005.01.016.

[73] J.M. Schultz, K.I. Jensen, Evacuated aerogel glazings, Vacuum. 82 (2008) 723–729. https://doi.org/10.1016/j.vacuum.2007.10.019.

[74] C. Buratti, E. Moretti, Experimental performance evaluation of aerogel glazing systems, Applied Energy. 97 (2012) 430–437. https://doi.org/10.1016/j.apenergy.2011.12.055.

[75] C. Buratti, E. Moretti, Glazing systems with silica aerogel for energy savings in buildings, Applied Energy. 98 (2012) 396–403. https://doi.org/10.1016/j.apenergy.2012.03.062.

[76] Y. Lv, R. Huang, H. Wu, S. Wang, X. Zhou, Study on Thermal and Optical Properties and Influence Factors of Aerogel Glazing Units, Procedia Engineering. 205 (2017) 3228–3234. https://doi.org/10.1016/j.proeng.2017.10.295.

[77] Y. Lv, H. Wu, Y. Liu, Y. Huang, T. Xu, X. Zhou, R. Huang, Quantitative research on the influence of particle size and filling thickness on aerogel glazing performance, Energy and Buildings. 174 (2018) 190–198. https://doi.org/10.1016/j.enbuild.2018.06.026.

[78] E. Moretti, E. Belloni, F. Merli, M. Zinzi, C. Buratti, Laboratory and pilot scale characterization of granular aerogel glazing systems, Energy and Buildings. 202 (2019) 1–15. https://doi.org/10.1016/j.enbuild.2019.109349.

[79] J.S. Carlos, H. Corvacho, P.D. Silva, J.P. Castro-Gomes, Heat recovery versus solar collection in a ventilated double window, Applied Thermal Engineering. 37 (2012) 258–266. https://doi.org/10.1016/j.applthermaleng.2011.11.027.

[80] J.S. Carlos, H. Corvacho, Ventilated Double Window for the Preheating of the Ventilation Air Comparison of Its Performance in a Northern and a Southern European Climate, Journal of Renewable Energy. 2013 (2013) 1–11. https://doi.org/10.1155/2013/290865.

[81] J.S. Carlos, H. Corvacho, P.D. Silva, J.P. Castro-Gomes, Modelling and simulation of a ventilated double window, Applied Thermal Engineering. 31 (2011) 93–102. https://doi.org/10.1016/j.applthermaleng.2010.08.021.

[82] S.A. Barakat, Thermal Performance of a Supply-Air Window, 12th Annual Passive Solar Conference. 12 (1987) 152–158.

[83] F. Khalvati, A. Omidvar, Summer study on thermal performance of an exhausting airflow window in evaporatively-cooled buildings, Applied Thermal Engineering. 153 (2019) 147–158. https://doi.org/10.1016/j.applthermaleng.2019.02.135.

[84] J. Wei, J. Zhao, Q. Chen, Energy performance of a dual airflow window under different climates, Energy and Buildings. 42 (2010) 111–122. https://doi.org/10.1016/j.enbuild.2009.07.018.

[85] J. Wei, J. Zhao, Q. Chen, Optimal design for a dual-airflow window for different climate regions in China, Energy and Buildings. 42 (2010) 2200–2205. https://doi.org/10.1016/j.enbuild.2010.07.016.

[86] V. Leal, E. Maldonado, The role of the PASLINK test cell in the modelling and integrated simulation of an innovative window, Building and Environment. 43 (2008) 217–227. https://doi.org/10.1016/j.buildenv.2006.10.025.

[87] T. Chow, Z. Lin, W. He, A.L.S. Chan, K.F. Fong, Use of ventilated solar screen window in warm climate, Applied Thermal Engineering. 26 (2006) 1910–1918. https://doi.org/10.1016/j.applthermaleng.2006.01.026.

[88] T. Chow, Z. Lin, K. fai Fong, L. Chan, M. miao He, Thermal performance of natural airflow window in subtropical and temperate climate zones - A comparative study, Energy Conversion and Management. 50 (2009) 1884–1890. https://doi.org/10.1016/j.enconman.2009.04.028.

[89] T. Chow, Z. Qiu, C. Li, Potential application of “see-through” solar cells in ventilated glazing in Hong Kong, Solar Energy Materials and Solar Cells. 93 (2009) 230–238. https://doi.org/10.1016/j.solmat.2008.10.002.

[90] W. Guo, L. Kong, T. Chow, C. Li, Q. Zhu, Z. Qiu, L. Li, Y. Wang, S.B. Riffat, Energy performance of photovoltaic (PV) windows under typical climates of China in terms of transmittance and orientation, Energy. 213 (2020) 118794. https://doi.org/10.1016/j.energy.2020.118794.

[91] T. Chow, C. Li, Z. Lin, Innovative solar windows for cooling-demand climate, Solar Energy Materials and Solar Cells. 94 (2010) 212–220. https://doi.org/10.1016/j.solmat.2009.09.004.

[92] T. Chow, C. Li, Z. Lin, The function of solar absorbing window as water-heating device, Building and Environment. 46 (2011) 955–960. https://doi.org/10.1016/j.buildenv.2010.10.027.

[93] C. Li, T. Chow, Water-filled double reflective window and its year-round performance, Procedia Environmental Sciences. 11 (2011) 1039–1047. https://doi.org/10.1016/j.proenv.2011.12.158.

[94] T. Chow, Y. Lyu, Effect of design configurations on water flow window performance, Solar Energy. 155 (2017) 354–362. https://doi.org/10.1016/j.solener.2017.06.050.

[95] Y. Lyu, X. Wu, C. Li, H. Su, L. He, Numerical analysis on the effectiveness of warm water supply in water flow window for room heating, Solar Energy. 177 (2019) 347–354. https://doi.org/10.1016/j.solener.2018.11.033.

[96] Y. Lyu, T. Chow, Evaluation of influence of header design on water flow characteristics in window cavity with CFD, Energy Procedia. 78 (2015) 97–102. https://doi.org/10.1016/j.egypro.2015.11.121.

[97] C. Liu, Y. Lyu, C. Li, J. Li, K. Zhuo, H. Su, Thermal performance testing of triple-glazing water flow window in cooing operation, Solar Energy. 218 (2021) 108–116. https://doi.org/10.1016/j.solener.2021.02.048.

[98] J. Stopper, M. Arch, F. Boeing, D. Gstoehl, Fluid Glass Façade Elements: Energy Balance of an Office Space with a Fluid Glass Façade, Proceedings of the Conference Sb13 Munich-Implementing Sustainability-Barriers and Chances. Munich. (2013). https://mediatum.ub.tum.de/doc/1251323/file.pdf.

[99] U. Berardi, The development of a monolithic aerogel glazed window for an energy retrofitting project, Applied Energy. 154 (2015) 603–615. https://doi.org/10.1016/j.apenergy.2015.05.059.

[100] C. Buratti, E. Moretti, E. Belloni, M. Zinzi, Experimental and numerical energy assessment of a monolithic aerogel glazing unit for building applications, Applied Sciences (Switzerland). 9 (2019). https://doi.org/10.3390/app9245473.

[101] H. Wang, H. Wu, Y. Ding, J. Feng, S. Wang, Feasibility and optimization of aerogel glazing system for building energy efficiency in different climates, International Journal of Low-Carbon Technologies. 10 (2015) 412–419. https://doi.org/10.1093/ijlct/ctu010.

[102] Y. Huang, J. lei Niu, Application of super-insulating translucent silica aerogel glazing system on commercial building envelope of humid subtropical climates - Impact on space cooling load, Energy. 83 (2015) 316–325. https://doi.org/10.1016/j.energy.2015.02.027.

[103] C.K. Leung, L. Lu, Y. Liu, H.S. Cheng, J.H. Tse, Optical and thermal performance analysis of aerogel glazing technology in a commercial building of Hong Kong, Energy and Built Environment. 1 (2020) 215–223. https://doi.org/10.1016/j.enbenv.2020.02.001.

[104] T. Gao, T. Ihara, S. Grynning, B.P. Jelle, A.G. Lien, Perspective of aerogel glazings in energy efficient buildings, Building and Environment. 95 (2016) 405–413. https://doi.org/10.1016/j.buildenv.2015.10.001.

[105] C. Buratti, E. Moretti, M. Zinzi, High energy-efficientwindows with silica aerogel for building refurbishment: Experimental characterization and preliminary simulations in

different climate conditions, Buildings. 7 (2017). https://doi.org/10.3390/buildings7010008.

[106] Y. Chen, Y. Xiao, S. Zheng, Y. Liu, Y. Li, Dynamic heat transfer model and applicability evaluation of aerogel glazing system in various climates of China, Energy. 163 (2018) 1115–1124. https://doi.org/10.1016/j.energy.2018.08.158.

[107] E. Belloni, C. Buratti, F. Merli, E. Moretti, T. Ihara, Energy & Buildings Thermal-energy and lighting performance of aerogel glazings with hollow silica : Field experimental study and dynamic simulations, Energy & Buildings. 243 (2021) 110999. https://doi.org/10.1016/j.enbuild.2021.110999.

[108] F. Goia, M. Perino, V. Serra, Improving thermal comfort conditions by means of PCM glazing systems, Energy and Buildings. 60 (2013) 442–452. https://doi.org/10.1016/j.enbuild.2013.01.029.

[109] K. Zhong, S. Li, G. Sun, S. Li, X. Zhang, Simulation study on dynamic heat transfer performance of PCM-filled glass window with different thermophysical parameters of phase change material, Energy and Buildings. 106 (2015) 87–95. https://doi.org/10.1016/j.enbuild.2015.05.014.

[110] D. Li, Z. Li, Y. Zheng, C. Liu, A.K. Hussein, X. Liu, Thermal performance of a PCM-filled double-glazing unit with different thermophysical parameters of PCM, Solar Energy. 133 (2016) 207–220. https://doi.org/10.1016/j.solener.2016.03.039.

[111] D. Li, T. Ma, C. Liu, Y. Zheng, Z. Wang, X. Liu, Thermal performance of a PCM-filled double glazing unit with different optical properties of phase change material,

Energy and Buildings. 119 (2016) 143–152. https://doi.org/10.1016/j.enbuild.2016.03.036.

[112] C. Liu, Y. Wu, D. Li, Y. Zhou, Z. Wang, X. Liu, Effect of PCM thickness and melting temperature on thermal performance of double glazing units, Journal of Building Engineering. 11 (2017) 87–95. https://doi.org/10.1016/j.jobe.2017.04.005.

[113] H. Hua, X. Wang, Y. Liu, Y. Ma, G. Li, L. Bi, Comparative study on dynamic heat transfer characteristics of CaCl2·6H2O and Na2SO4·10H2O used in PCM-filled glass window, Science and Technology for the Built Environment. 25 (2019) 905–913. https://doi.org/10.1080/23744731.2019.1565552.

[114] A.M. Bolteya, M.A. Elsayad, A.M. Belal, Thermal efficiency of PCM filled double glazing units in Egypt, Ain Shams Engineering Journal. (2021). https://doi.org/10.1016/j.asej.2020.12.004.

[115] D. Li, Y. Wu, C. Liu, G. Zhang, M. Arıcı, Energy investigation of glazed windows containing Nano-PCM in different seasons, Energy Conversion and Management. 172 (2018) 119–128. https://doi.org/10.1016/j.enconman.2018.07.015.

[116] A. Wieprzkowicz, D. Heim, Modelling of thermal processes in a glazing structure with temperature dependent optical properties - An example of PCM-window, Renewable Energy. 160 (2020) 653–662. https://doi.org/10.1016/j.renene.2020.06.146.

[117] S. Zhang, W. Hu, D. Li, C. Zhang, M. Arıcı, Ç. Yıldız, X. Zhang, Y. Ma, Energy efficiency optimization of PCM and aerogel-filled multiple glazing windows, Energy. 222 (2021). https://doi.org/10.1016/j.energy.2021.119916.

[118] Y. Huang, J.L. Niu, Energy and visual performance of the silica aerogel glazing system in commercial buildings of Hong Kong, Construction and Building Materials. 94 (2015) 57–72. https://doi.org/10.1016/j.conbuildmat.2015.06.053.